



CERN-EP-2023-078  
 LHCb-PAPER-2022-047  
 August 29, 2023

# Associated production of prompt $J/\psi$ and $\Upsilon$ mesons in $pp$ collisions at $\sqrt{s} = 13$ TeV

LHCb collaboration<sup>†</sup>

## Abstract

The associated production of prompt  $J/\psi$  and  $\Upsilon$  mesons in  $pp$  collisions at a centre-of-mass energy of  $\sqrt{s} = 13$  TeV is studied using LHCb data, corresponding to an integrated luminosity of  $4\text{ fb}^{-1}$ . The measurement is performed for  $J/\psi$  ( $\Upsilon$ ) mesons with a transverse momentum  $p_T < 10$  (30) GeV/ $c$  in the rapidity range  $2.0 < y < 4.5$ . In this kinematic range, the cross-section of the associated production of prompt  $J/\psi$  and  $\Upsilon(1S)$  mesons is measured to be  $133 \pm 22 \pm 7 \pm 3\text{ pb}$ , with a significance of  $7.9\sigma$ , and that of prompt  $J/\psi$  and  $\Upsilon(2S)$  mesons to be  $76 \pm 21 \pm 4 \pm 7\text{ pb}$ , with a significance of  $4.9\sigma$ . The first uncertainty is statistical, the second systematic, and the third due to uncertainties on the used branching fractions. This is the first observation of the associated production of  $J/\psi$  and  $\Upsilon(1S)$  in proton-proton collisions. Differential cross-sections are measured as functions of variables that are sensitive to kinematic correlations between the  $J/\psi$  and  $\Upsilon(1S)$  mesons. The effective cross-sections of the associated production of prompt  $J/\psi$  and  $\Upsilon$  mesons are obtained and found to be compatible with measurements using other particle productions.

Published in JHEP 08 (2023) 093

© 2023 CERN for the benefit of the LHCb collaboration. CC BY 4.0 licence.

---

<sup>†</sup>Authors are listed at the end of this paper.



# 1 Introduction

Hadroproduction of heavy quarkonia has been extensively studied to probe quantum chromodynamics (QCD) [1]. Various theoretical treatments have been proposed that model the production of quark-antiquark pairs  $Q\bar{Q}$  and their subsequent hadronisation into quarkonia. Promising approaches include the colour-singlet model (CSM) [2–4] and the non-relativistic QCD (NRQCD) framework [5]. The CSM considers only the colour-singlet intermediate  $Q\bar{Q}$  state with the same  $J^{PC}$  quantum numbers as the final-state quarkonium, while the NRQCD framework considers both colour-singlet and colour-octet  $Q\bar{Q}$  states. The NRQCD framework assumes process-independent long-distance matrix elements (LDMEs) to describe the transition probabilities from the intermediate  $Q\bar{Q}$  states to the final-state quarkonium. Quarkonium hadroproduction cross-sections as a function of the transverse momentum ( $p_T$ ) are successfully described by NRQCD calculations [6–11]. However, there are still challenges in providing a coherent description of all heavy quarkonium hadroproduction data, *e.g.* there is no unified description of the cross-sections and polarisation of the vector quarkonium states; and the inconsistency between the LDMEs of the  $\eta_c$  and  $J/\psi$  states—which are related to the heavy-quark spin symmetry—remains to be understood [12–19].

In hadron collisions, a pair of heavy quarkonia can be produced through either single-parton scattering (SPS), or double-parton scattering (DPS), depending on the number of parton-parton scatterings in the process. A representative Feynman diagram of each process is presented in Fig. 1. In the SPS process, two quarkonia are produced in the same parton-parton interaction, leading to kinematic correlations between them. In contrast, two parton-parton interactions occur simultaneously and independently in the DPS process, producing two quarkonia with weak kinematic correlations. While the SPS process provides new insights into the heavy quarkonium production mechanism according to the left Feynman diagram in Fig. 1 [20–23], the DPS process probes the parton distribution function inside the colliding hadrons and provides valuable information on the hadronic wave functions describing correlations among partons [1]. Taking the  $J/\psi$  and  $\Upsilon$  associated production (referred to as  $J/\psi$ - $\Upsilon$  production throughout) as an example<sup>1</sup>, the DPS cross-section  $\sigma_{\text{DPS}}(J/\psi\text{-}\Upsilon)$  can be estimated from the  $J/\psi$  and  $\Upsilon$  cross-sections,

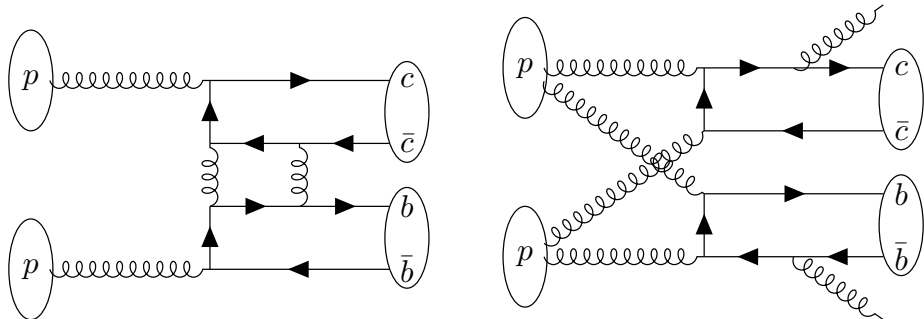


Figure 1: Representative Feynman diagrams of the (left) SPS and the (right) DPS process with colour-singlet LDMEs.

<sup>1</sup>Throughout the paper,  $\Upsilon$  represents  $\Upsilon(1S)$ ,  $\Upsilon(2S)$ , or  $\Upsilon(3S)$ .

$\sigma(J/\psi)$  and  $\sigma(\Upsilon)$ , as

$$\sigma_{\text{DPS}}(J/\psi-\Upsilon) = \frac{\sigma(J/\psi) \times \sigma(\Upsilon)}{\sigma_{\text{eff}}}, \quad (1)$$

where  $\sigma_{\text{eff}}$  is the effective cross-section parameter encoding the transverse overlapping region between partons in the protons [24–26]. The effective cross-section is expected to be universal based on the assumptions that the two sets of colliding partons are uncorrelated and the longitudinal and transverse components of the parton distribution function factorise. Measurements in different processes for the effective cross-section are mostly within the range of 5 to 35 mb [27, 28]. Further study is needed to test its universality [29].

A range of associated production processes of heavy quarkonia has been studied experimentally [20, 28, 30–42]. Heavy-quarkonium-pair production was first observed by the NA3 collaboration in the study of  $J/\psi$ -pair production in  $\pi^-$ -induced interactions [43]. Subsequently,  $J/\psi$ -pair production was measured by the LHCb experiment [44] and the CMS experiment [45] at  $\sqrt{s} = 7$  TeV, by the D0 collaboration at  $\sqrt{s} = 1.96$  TeV in  $p\bar{p}$  collisions [33], by the ATLAS experiment at  $\sqrt{s} = 8$  TeV [34], and by the LHCb experiment at  $\sqrt{s} = 13$  TeV [46]. In the di- $J/\psi$  invariant-mass spectrum, a structure of fully charmed tetraquark states was observed by LHCb [47], and recently confirmed by CMS [48] and ATLAS [49]. Production of  $\Upsilon$  pairs was observed by the CMS experiment in  $pp$  collisions at  $\sqrt{s} = 8$  TeV [50]. For  $J/\psi-\Upsilon$  production, experimental evidence was found by the D0 collaboration [51], but to date, no significant signals have been reported.

In this paper,  $J/\psi-\Upsilon$  production in  $pp$  collisions at a centre-of-mass energy of  $\sqrt{s} = 13$  TeV is studied for  $J/\psi$  ( $\Upsilon$ ) mesons with a transverse momentum  $p_T < 10$  (30) GeV/ $c$  in the rapidity range  $2.0 < y < 4.5$  using data collected by LHCb in the years 2016, 2017, and 2018. The data correspond to an integrated luminosity of  $\mathcal{L} = 4.18 \pm 0.08 \text{ fb}^{-1}$ . The  $J/\psi$  and  $\Upsilon$  mesons are reconstructed in the dimuon final state. The polarisation of the  $J/\psi$  and  $\Upsilon$  mesons is assumed to be zero. The polarisation of  $J/\psi-\Upsilon$  pairs is not yet measured, but all the LHC measurements so far indicate a small polarisation for quarkonia [52–57].

## 2 Detector and dataset

The LHCb detector [58, 59] is a single-arm forward spectrometer covering the pseudorapidity range  $2 < \eta < 5$ , designed for the study of particles containing  $b$  or  $c$  quarks. The detector includes a high-precision tracking system consisting of a silicon-strip vertex detector surrounding the  $pp$  interaction region, a large-area silicon-strip detector located upstream of a dipole magnet with a bending power of about 4 Tm, and three stations of silicon-strip detectors and straw drift tubes placed downstream of the magnet. The tracking system provides a measurement of the momentum,  $p$ , of charged particles with a relative uncertainty that varies from 0.5% at low momentum to 1.0% at 200 GeV/ $c$ . The minimum distance of a track to a primary  $pp$  collision vertex (PV), the impact parameter, is measured with a resolution of  $(15 + 29/p_T) \mu\text{m}$ , where  $p_T$  is in GeV/ $c$ . Particle identification (PID) for charged hadrons uses information from two ring-imaging Cherenkov detectors. Photons, electrons and hadrons are identified by a calorimeter system consisting of scintillating-pad and preshower detectors, an electromagnetic and a hadronic calorimeter. Muons are identified by a system composed of alternating layers of iron and multiwire proportional chambers.

The online event selection is performed by a trigger [60], which consists of a hardware stage, based on information from the calorimeter and muon systems, followed by a software stage, which applies a full event reconstruction. For this analysis, data were collected with varying trigger conditions particularly for the hardware stage, which requires two muons with  $p_T(\mu_1) \times p_T(\mu_2) > (1.3)^2, (1.5)^2$  or  $(1.8)^2 \text{ GeV}^2/c^2$ . In the software trigger stage, at least two muons with  $p_T > 300 \text{ MeV}/c$ ,  $p > 6 \text{ GeV}/c$ , and dimuon invariant mass  $m(\mu^+\mu^-) > 2.7 \text{ GeV}/c^2$  are required. Candidate  $J/\psi$  and  $\Upsilon$  mesons are built from two oppositely charged tracks that are identified as muons and form a good vertex. These muons from the  $J/\psi$  ( $\Upsilon$ ) decays are required to be in the kinematic region  $2 < \eta < 5$ ,  $p_T > 650$  (3000)  $\text{MeV}/c$ , and  $p > 6 \text{ GeV}/c$ . The decay vertices of the  $J/\psi$  and  $\Upsilon$  mesons have to be consistent with the same PV. The invariant mass of the  $J/\psi$  candidates is required to be within  $[3.0, 3.2] \text{ GeV}/c^2$  and that of the  $\Upsilon$  candidates within  $[9, 11] \text{ GeV}/c^2$ .

Two independent simulated samples of  $J/\psi$  and  $\Upsilon$  decays are used to model effects of the detector acceptance and the imposed selection requirements for  $J/\psi$  and  $\Upsilon$  decays respectively. Primary  $pp$  collisions are generated using Pythia 8 [61] with a specific LHCb configuration [62]. Decays of unstable particles are simulated using EvtGen [63], in which the final-state radiation is generated with PHOTOS [64]. The interaction of the generated particles with the detector, and its response, are implemented using the GEANT4 toolkit [65] as described in Ref. [66]. All simulated events are reconstructed and selected in the same way as the data.

### 3 Cross-section determination

The  $J/\psi$ - $\Upsilon$  production cross-section is measured according to

$$\sigma(J/\psi\text{-}\Upsilon) = \frac{N_{\text{cor}}}{\mathcal{L} \times \mathcal{B}_{J/\psi \rightarrow \mu^+\mu^-} \times \mathcal{B}_{\Upsilon \rightarrow \mu^+\mu^-}}, \quad (2)$$

where  $N_{\text{cor}}$  is the efficiency-corrected signal yield of the  $J/\psi$ - $\Upsilon$  associated production,  $\mathcal{B}_{J/\psi \rightarrow \mu^+\mu^-}$  and  $\mathcal{B}_{\Upsilon \rightarrow \mu^+\mu^-}$  are the branching fractions of the  $J/\psi \rightarrow \mu^+\mu^-$  and  $\Upsilon \rightarrow \mu^+\mu^-$  decays [67], respectively, and  $\mathcal{L} = 4.18 \pm 0.08 \text{ fb}^{-1}$  is the integrated luminosity determined with the van-der-Meer-scan method [68, 69].

The total detection efficiency  $\epsilon_{\text{tot}}$  for the offline selected  $J/\psi$ - $\Upsilon$  candidates is factorised as

$$\epsilon_{\text{tot}} = \epsilon_{\text{acc}} \times \epsilon_{\text{rec\&sel}} \times \epsilon_{\text{PID}} \times \epsilon_{\text{trig}}, \quad (3)$$

where  $\epsilon_{\text{acc}}$  is the geometrical acceptance,  $\epsilon_{\text{rec\&sel}}$  is the reconstruction and selection (not including PID requirements) efficiency of all the candidates within the geometrical acceptance,  $\epsilon_{\text{PID}}$  is the PID selection efficiency of candidates reconstructed and passing other selection requirements, and  $\epsilon_{\text{trig}}$  is the trigger selection efficiency of candidates passing all selection requirements. The first three terms on the right-hand side of Eq. 3 are computed by multiplying the individual efficiencies for  $J/\psi$  and  $\Upsilon$  candidates, *i.e.*,

$$\epsilon_i = \epsilon_i^{J/\psi} \times \epsilon_i^{\Upsilon}, \quad (4)$$

where  $i$  denotes acc, rec&sel, or PID. For the trigger selection, it is required that either the  $J/\psi$  or  $\Upsilon$  candidate meets the trigger requirements specified in Sec. 2; therefore the trigger efficiency  $\epsilon_{\text{trig}}$  can be factorised as

$$\epsilon_{\text{trig}} = 1 - (1 - \epsilon_{\text{trig}}^{J/\psi})(1 - \epsilon_{\text{trig}}^{\Upsilon}). \quad (5)$$

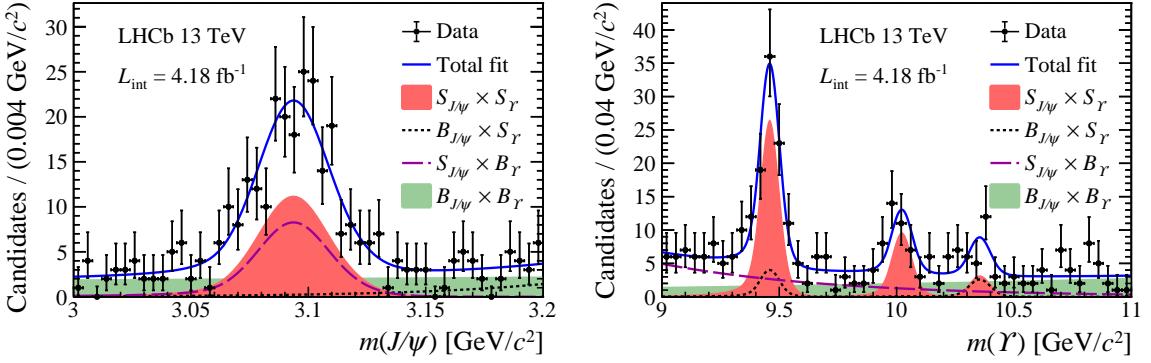


Figure 2: Two-dimensional invariant mass distribution of the  $J/\psi$ - $\Upsilon$  candidates projected on (left) the  $J/\psi$  invariant mass  $m(J/\psi)$  and (right) the  $\Upsilon$  invariant mass  $m(\Upsilon)$ . The black points with error bars represent the data. The blue solid line represents the result of the fit to the data sample. The red shaded area represents the signal component. The black (dotted) and violet (dashed) lines represent the background where one dimuon candidate is a true meson decay and the other is combinatorial background. The green shaded area indicates the background where both the  $J/\psi$  and  $\Upsilon$  candidates are combinatorial background.

Each efficiency component is determined separately for  $J/\psi$  and  $\Upsilon$  mesons as a function of their  $p_T$  and rapidity  $y$ . The acceptances, the reconstruction and selection efficiencies, and the trigger efficiencies are estimated using simulation, while the PID efficiencies are obtained using a data-driven method [70].

To extract the signal yield, an unbinned extended maximum-likelihood fit is performed to the two-dimensional  $J/\psi$ - $\Upsilon$  invariant-mass distribution. Defining the signal distribution to be  $S$  and combinatorial-background distribution  $B$ , the components in the model used to fit the data fall into three categories, each corresponding to the following cases:

- the signal  $J/\psi$ - $\Upsilon$  candidates ( $S_{J/\psi} \times S_\Upsilon$ , in which  $S_\Upsilon$  is  $S_{\Upsilon(1S)} + S_{\Upsilon(2S)} + S_{\Upsilon(3S)}$ ),
- a true  $J/\psi$  ( $\Upsilon$ ) candidate associated with a combinatorial  $\Upsilon$  ( $J/\psi$ ) background candidate ( $S_{J/\psi} \times B_\Upsilon$  and  $B_{J/\psi} \times S_\Upsilon$ ),
- and a purely combinatorial background ( $B_{J/\psi} \times B_\Upsilon$ ).

The two-dimensional probability density function for each component factorises into the product of two one-dimensional distributions for the  $J/\psi$  and  $\Upsilon$  candidates. The signal invariant-mass distribution of the  $J/\psi$  meson and that of each  $\Upsilon$  meson are described by a combination of a double-sided Crystal Ball (DSCB) function [71] and a Gaussian function with a shared mean. The DSCB power-law tail parameters, the ratio of the width of the Gaussian function to that of the Gaussian core in the DSCB function, and the relative fraction of the DSCB to the Gaussian function are fixed to values estimated from simulation. The ratios between the means of the  $\Upsilon$  Gaussian functions are fixed to the ratios of the known  $\Upsilon$  masses. As the mass resolution of signals is linearly dependent on invariant mass, the width ratios of the Gaussian functions are also fixed to the known mass ratios [67]. The mean value and the width of the Gaussian function for the  $\Upsilon(1S)$  are free parameters in the fit.

Table 1: Raw yields from the fit, the efficiency-corrected yields ( $N_{\text{cor}}$ ) and the signal significances.

Signal	Raw yields	$N_{\text{cor}}$	Significances
$J/\psi-\Upsilon(1S)$	$76 \pm 12$	$840 \pm 140$	$7.9\sigma$
$J/\psi-\Upsilon(2S)$	$30 \pm 7$	$370 \pm 100$	$4.9\sigma$
$J/\psi-\Upsilon(3S)$	$10 \pm 6$	-	$1.7\sigma$

Each combinatorial background is modelled by an exponential function. The invariant-mass distributions of the  $J/\psi$  and  $\Upsilon$  candidates, together with the fit projections, are shown in Fig. 2. Associated  $J/\psi-\Upsilon(1S)$  production is observed with a significance of  $7.9\sigma$ , and evidence for  $J/\psi-\Upsilon(2S)$  production with a significance of  $4.9\sigma$  is seen. The total significance for the associated production of  $J/\psi$  with a combination of  $\Upsilon(1S)$ ,  $\Upsilon(2S)$ , and  $\Upsilon(3S)$  states is determined to be  $8.5\sigma$ . The significance is estimated by comparing the likelihood of the fit with and without the considered component in the fit, with relevant systematic uncertainties taken into consideration. The raw yields of signals from the fit and their significances are summarised in Table 1.

Based on the fit result, a signal weight  $w_i$  is calculated with the *sPlot* method [72] for each  $J/\psi-\Upsilon$  candidate, using the  $J/\psi$  and  $\Upsilon$  invariant masses as discriminating variables. These weights are used to determine the efficiency corrected yield  $N^{\text{cor}} = \sum_j w_j / \epsilon_{\text{tot},j}$ , where  $j$  runs over all the  $J/\psi-\Upsilon$  candidates in data. The total efficiency for the  $j^{\text{th}}$  candidate,  $\epsilon_{\text{tot},j}$ , is defined in Eq. 3 and determined as a function of the  $p_{\text{T}}$  and  $y$  of the  $J/\psi$  and  $\Upsilon$  candidate. The corrected yield,  $N_{\text{cor}}$ , is shown in Table 1.

The signal extracted from the fit also contains  $J/\psi$  mesons produced from  $b$ -hadron decays (denoted  $J/\psi$ -from- $b$ ). The fraction of  $J/\psi$ -from- $b$  decays is determined to be 2.1% using the prompt  $J/\psi$  and  $J/\psi$ -from- $b$  production cross-sections measured by LHCb in  $pp$  collisions at  $\sqrt{s} = 13$  TeV [73]. The difference between the average reconstruction and selection efficiencies of the two components is evaluated from simulation; the selection criteria constraining  $J/\psi$  and  $\Upsilon$  decay vertices to the PV favour the prompt  $J/\psi$  candidates and suppress the  $J/\psi$ -from- $b$  candidates. With current measurements of  $\sigma_{\text{eff}}$ , the  $J/\psi-\Upsilon$  associated production is predicted to be dominated by the DPS process. It is therefore assumed that in events with  $J/\psi$  and  $\Upsilon$  candidates the relative cross-section of the  $J/\psi$ -from- $b$  production with respect to the prompt  $J/\psi$  production is the same as the relative cross-section of  $J/\psi$ -from- $b$  in inclusive  $J/\psi$  events. An uncertainty is assigned for systematic effects due to this assumption. The  $J/\psi$ -from- $b$  component is subtracted when calculating the total cross-section of the associated  $J/\psi-\Upsilon$  production.

## 4 Systematic uncertainties

Systematic uncertainties from various sources are studied and summarised in Table 2. The total relative systematic uncertainty is 5.5% for  $J/\psi-\Upsilon(1S)$  and 10.3% for  $J/\psi-\Upsilon(2S)$  production, corresponding to the quadratic sum of all the contributions discussed below.

The uncertainty introduced by the imperfect modelling of the signal shape is estimated by fitting the data with an alternative signal model. The alternative shape is the shape of the simulated signal distribution, convolved with a Gaussian function to account for the different invariant-mass resolution observed between data and simulation. The 2.0% relative change of the signal yield is assigned as the systematic uncertainty for both

Table 2: Relative systematic uncertainties on the measurement of the  $J/\psi\text{-}\Upsilon(1S)$  and  $J/\psi\text{-}\Upsilon(2S)$  cross-sections.

Source	$\sigma(J/\psi\text{-}\Upsilon(1S))$ (%)	$\sigma(J/\psi\text{-}\Upsilon(2S))$ (%)
Signal shape	2.0	2.0
Limited simulation size	0.7	1.6
Tracking efficiency	3.3	3.3
PID efficiency	0.5	0.5
$J/\psi$ -from- $b$ fraction	1.1	1.1
Trigger efficiency	1.0	1.0
Radiative tail	2.0	2.0
Vertex fit	0.6	0.6
Luminosity	1.9	1.9
$\mathcal{B}_{J/\psi \rightarrow \mu^+ \mu^-}$	0.6	0.6
$\mathcal{B}_{\Upsilon(1S) \rightarrow \mu^+ \mu^-}$	2.0	—
$\mathcal{B}_{\Upsilon(2S) \rightarrow \mu^+ \mu^-}$	—	8.8
Total	5.5	10.3

$J/\psi\text{-}\Upsilon(1S)$  and  $J/\psi\text{-}\Upsilon(2S)$  signals.

Due to the limited sizes of the simulation samples, the efficiencies obtained from simulation are subject to fluctuations. The statistical uncertainties of the efficiencies are propagated to the efficiency-corrected signal yield with a pseudoexperiment Monte Carlo method. The variations of the efficiency-corrected signal yields in pseudoexperiments are taken as the systematic uncertainty and are 0.7% for  $J/\psi\text{-}\Upsilon(1S)$  production and 1.6% for  $J/\psi\text{-}\Upsilon(2S)$  production.

The track reconstruction efficiency as a function of muon  $p$  and  $\eta$  is estimated with  $J/\psi \rightarrow \mu^+ \mu^-$  decays in a calibration data sample using a tag-and-probe technique [74]. The difference between data and simulation is used to calibrate the reconstruction efficiency estimated using simulated signal decays. The uncertainties on these calibrations are propagated to the efficiency-corrected yield using a pseudoexperiment Monte Carlo method. The uncertainty is 0.9% for both the  $J/\psi\text{-}\Upsilon(1S)$  and  $J/\psi\text{-}\Upsilon(2S)$  signals. An additional uncertainty of 0.8% per track is assigned to account for the difference in detector occupancy between data and simulation [74]. A total relative uncertainty of 3.3% is attributed to the tracking efficiency calibration.

The muon PID efficiency is calculated with  $J/\psi \rightarrow \mu^+ \mu^-$  decays using a data-driven tag-and-probe method [70]. The efficiency is estimated in bins of  $p_T$  and  $\eta$  of the probe track, for which the binning scheme introduces an uncertainty. Alternative binning schemes are used to estimate variations of the PID efficiency. The relative change with respect to the default value, 0.5%, is quoted as the systematic uncertainty.

The trigger efficiency estimated from simulation is compared with that from data with a data-driven method [46, 75]. A relative difference of 1.0% is quoted as the systematic uncertainty.

The uncertainties introduced by the mismodelling of the radiative decay tails and the requirement on the vertex fit quality is estimated to be 2% and 0.6%, respectively, following Ref. [73, 76] by comparing data and simulation.

The fraction of  $J/\psi$ -from- $b$  is calculated from the  $p_T$ - and  $y$ -dependent  $J/\psi$ -from- $b$  fraction in single  $J/\psi$  production and the relative detection efficiency between  $J/\psi$ -from- $b$  and prompt production, convolved with the  $J/\psi$  kinematic distributions in simulation. The uncertainty of  $J/\psi$  kinematic distributions used to estimate the fraction and the possible difference of  $J/\psi$ -from- $b$  fraction between inclusive  $J/\psi$  production and associated  $J/\psi-\Upsilon$  production are sources of systematic uncertainties. The first uncertainty is evaluated using the maximum and minimum values of the inclusive  $J/\psi$ -from- $b$  fraction in the studied kinematic range of this analysis. The second source is estimated conservatively by varying the effective cross-section  $\sigma_{\text{eff}}$  of the  $\Upsilon-B$  hadron associated production by 50%. In total, this systematic uncertainty is estimated to be 1.1%. The effect of events where  $J/\psi$  and  $\Upsilon$  mesons originate from different PVs is estimated to be negligible.

The relative uncertainty on the luminosity is estimated to be 1.9%. The relative uncertainties on the branching fractions  $\mathcal{B}_{J/\psi \rightarrow \mu^+ \mu^-}$ ,  $\mathcal{B}_{\Upsilon(1S) \rightarrow \mu^+ \mu^-}$  and  $\mathcal{B}_{\Upsilon(2S) \rightarrow \mu^+ \mu^-}$  are 0.6%, 2.0% and 8.8%, respectively [67]. They are propagated to the cross-section uncertainties.

## 5 Results and comparison to theory

The  $J/\psi-\Upsilon$  production is measured in the fiducial region,  $2 < y < 5$  and  $p_T < 10 \text{ GeV}/c$  for the  $J/\psi$  meson,  $2 < y < 5$  and  $p_T < 30 \text{ GeV}/c$  for the  $\Upsilon$  meson. The associated prompt-production cross-section of  $J/\psi-\Upsilon(1S)$  is measured to be

$$\sigma(J/\psi-\Upsilon(1S)) = 133 \pm 22 \pm 7 \pm 3 \text{ pb},$$

and the associated prompt-production cross-section of  $J/\psi-\Upsilon(2S)$  is measured to be

$$\sigma(J/\psi-\Upsilon(2S)) = 76 \pm 21 \pm 4 \pm 7 \text{ pb},$$

where the first uncertainties are statistical, the second systematic, and the third due to the uncertainties on the quarkonium decay branching fractions.

The ratio of the cross-sections of  $J/\psi-\Upsilon(2S)$  and  $J/\psi-\Upsilon(1S)$  multiplied by the respective branching ratio is calculated to be

$$\frac{\mathcal{B}_{\Upsilon(2S) \rightarrow \mu^+ \mu^-} \times \sigma(J/\psi-\Upsilon(2S))}{\mathcal{B}_{\Upsilon(1S) \rightarrow \mu^+ \mu^-} \times \sigma(J/\psi-\Upsilon(1S))} = 0.442 \pm 0.143 \pm 0.004,$$

where the first uncertainty is statistical and the second systematic. The result is consistent with the measurement of  $\Upsilon(1S, 2S)$  production [76] and of the production of  $\Upsilon(1S, 2S)$  mesons associated with an open charm hadron [38], as is expected by the DPS assumption.

Using the DPS cross-section of the  $J/\psi-\Upsilon$  associated production and the prompt-production cross-sections of single  $J/\psi$  and  $\Upsilon$  mesons, the effective cross-section is calculated according to Eq. 1. The DPS cross-sections are estimated by subtracting the SPS cross-sections,  $20^{+52}_{-15} \text{ pb}$  for  $J/\psi-\Upsilon(1S)$  and  $8^{+22}_{-6} \text{ pb}$  for  $J/\psi-\Upsilon(2S)$ , from the associated-production cross-sections. The SPS cross-sections are adapted from the calculations with the NRQCD framework in Ref. [20]. The prompt-production cross-sections of  $J/\psi$  and  $\Upsilon$  are taken from Ref. [73] and Ref. [76], respectively. The effective cross-section is

$$\sigma_{\text{eff}}(J/\psi-\Upsilon(1S)) = 26 \pm 5 \pm 2^{+22}_{-3} \text{ mb},$$

$$\sigma_{\text{eff}}(J/\psi-\Upsilon(2S)) = 14 \pm 5 \pm 1^{+7}_{-1} \text{ mb},$$

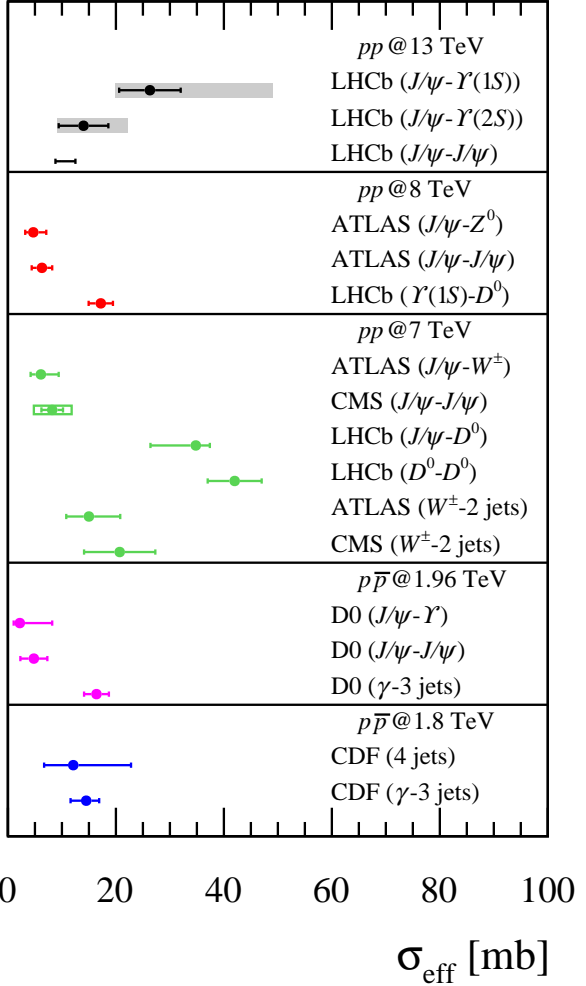


Figure 3: Effective cross-sections measured in different particle production by various experiments. For the LHCb measurements of  $J/\psi - \Upsilon(1S)$  and  $J/\psi - \Upsilon(2S)$  effective cross-sections, the error bars (grey boxes) represent the experimental (total) uncertainties. The result for  $J/\psi - J/\psi$  production at LHCb is given as a range covering several model-dependent measurements [46]. Results from other analyses are reproduced from Refs. [1, 38].

where the first uncertainties are statistical, the second uncertainties are systematic, and the last terms are uncertainties due to theory calculations. The results of  $\sigma_{\text{eff}}$  are broadly compatible with measurements using hadroproduction of other particles, as shown in Fig. 3. The effective cross-sections for  $J/\psi - \Upsilon(1S)$  and  $J/\psi - \Upsilon(2S)$  production are consistent.

The distributions of some observables related to both  $J/\psi$  and  $\Upsilon(1S)$  mesons are studied to probe the kinematic correlation between the two mesons. These variables include the  $J/\psi - \Upsilon(1S)$  invariant mass, the transverse momentum of the  $J/\psi - \Upsilon(1S)$  system, the relative azimuthal angle, and the rapidity difference between  $J/\psi$  and  $\Upsilon(1S)$  mesons. The distributions of these variables and the transverse momentum distributions of the  $J/\psi$  and  $\Upsilon(1S)$  mesons are presented in Fig. 4, after correcting for the total detection efficiency and subtracting the background contribution. The large uncertainties in the correlation distributions are due to the small size of the signal data sample, which dominate over systematic uncertainties. These distributions are compared with pseudoexperiments corresponding to different contributions of the DPS and SPS processes. Since the  $J/\psi$  and  $\Upsilon$  mesons are produced independently from two different parton-parton scatterings in the DPS processes, the kinematic distribution of each meson in the associated production

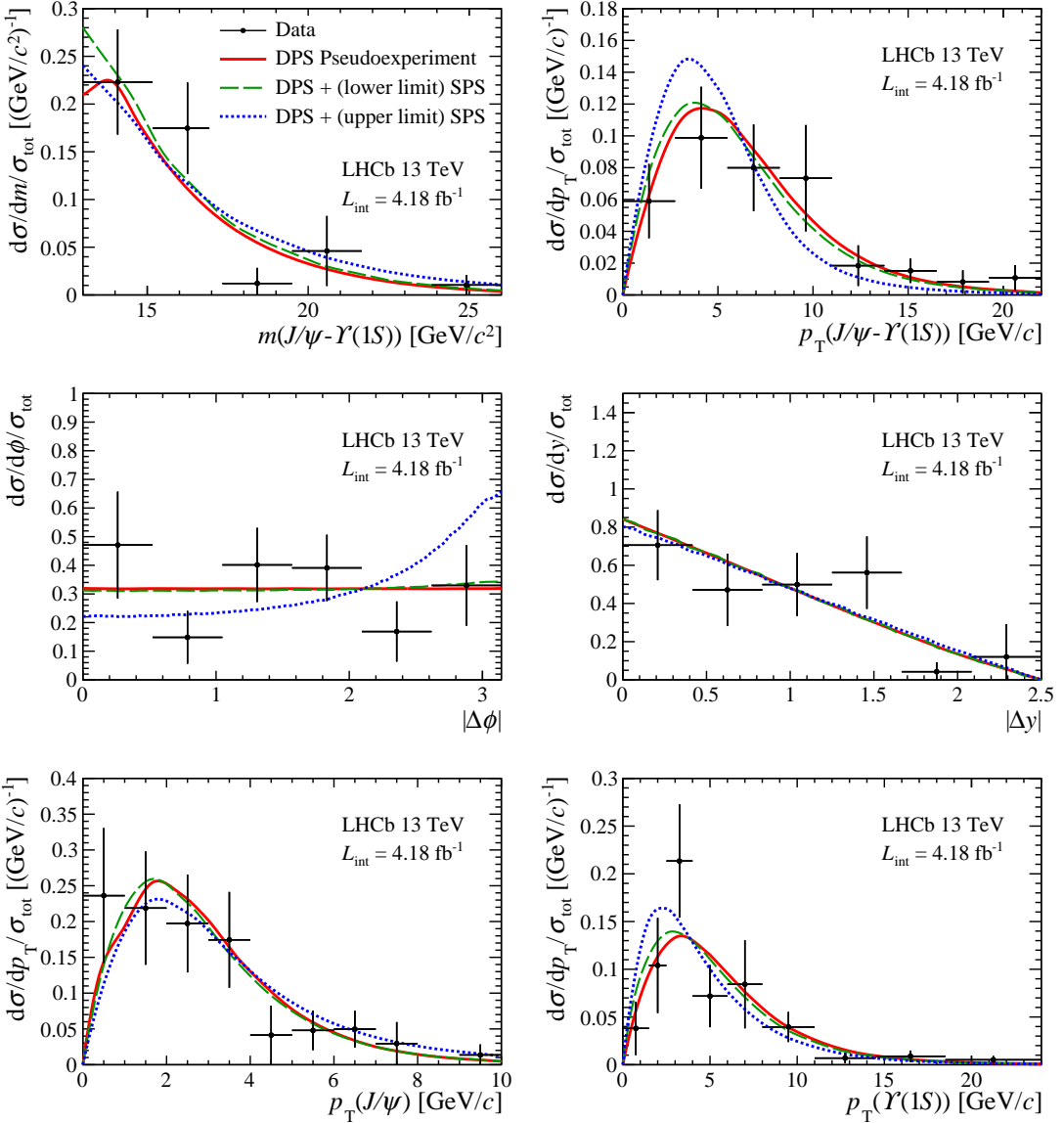


Figure 4: Distributions of (top left) invariant mass  $m(J/\psi-\Upsilon(1S))$ , (top right) transverse momentum  $p_T(J/\psi-\Upsilon(1S))$ , (middle left) azimuthal angle difference  $|\Delta\phi|$ , (middle right) rapidity difference  $|\Delta y|$  of  $J/\psi-\Upsilon(1S)$ , and (bottom)  $p_T$  of the  $J/\psi$  and  $\Upsilon(1S)$  mesons for data and the pseudodata modelled from previous measurements [73, 76]. Black points with error bars represent the data distributions with statistical uncertainties. Red solid lines represent distributions of the DPS pseudodata. Green dashed lines and blue dotted lines represent the DPS distribution together with the lower limit and the upper limit of the SPS distributions, respectively.

is expected to be similar to that in the single meson production. As a result, using the measured  $p_T$  and  $y$  distributions in single- $J/\psi$  and  $-\Upsilon(1S)$  production [73, 76], the DPS distributions of  $J/\psi$  and  $\Upsilon(1S)$  kinematic variables in the associated production can be modelled. The distributions for the SPS production are taken from calculations in Ref. [20]. Three samples of pseudodata are generated, differing in the relative SPS to DPS fractions. For one sample, only DPS production is considered. For the other two samples, the SPS fraction is calculated using either the upper or lower limit of the

predicted cross-section in Ref. [20], and the DPS cross-section is the LHCb measurement of the total cross-section with the SPS cross-section subtracted. As shown in Fig. 4, the  $J/\psi$  and  $\Upsilon(1S)$   $p_T$  distributions and the kinematic correlations between the  $J/\psi$  and  $\Upsilon(1S)$  mesons in the three pseudodata samples are all found to be consistent with measurements.

## 6 Summary

Using  $pp$  collision data collected by the LHCb experiment at a centre-of-mass energy of 13 TeV corresponding to an integrated luminosity of  $4.18 \pm 0.08 \text{ fb}^{-1}$ , a signal for  $J/\psi$ - $\Upsilon(1S)$  production is observed with a significance of  $7.9\sigma$ , and evidence is found for  $J/\psi$ - $\Upsilon(2S)$  production. Within the fiducial region  $2.0 < y < 4.5$  and  $p_T < 10$  (30) GeV/ $c$  for  $J/\psi$  ( $\Upsilon$ ) mesons, the cross-section for  $J/\psi$ - $\Upsilon(1S)$  production is measured to be  $133 \pm 22$  (stat)  $\pm 7$  (syst)  $\pm 3$  ( $\mathcal{B}$ ) pb and that for  $J/\psi$ - $\Upsilon(2S)$  production  $76 \pm 21$  (stat)  $\pm 4$  (syst)  $\pm 7$  ( $\mathcal{B}$ ) pb. The effective cross-sections for  $J/\psi$ - $\Upsilon(1S)$  and  $J/\psi$ - $\Upsilon(2S)$  production are calculated and found to be compatible with previous measurements in various processes. Kinematic correlations between the  $J/\psi$  and  $\Upsilon(1S)$  mesons are studied, showing results consistent with both the hypotheses that the associated production is dominated by the DPS process or has DPS and SPS contributions. In the future, further data from LHCb combined with improved theory calculations will help constrain the associated quarkonium production mechanism.

## Acknowledgements

We express our gratitude to our colleagues in the CERN accelerator departments for the excellent performance of the LHC. We thank the technical and administrative staff at the LHCb institutes. We acknowledge support from CERN and from the national agencies: CAPES, CNPq, FAPERJ and FINEP (Brazil); MOST and NSFC (China); CNRS/IN2P3 (France); BMBF, DFG and MPG (Germany); INFN (Italy); NWO (Netherlands); MNiSW and NCN (Poland); MEN/IFA (Romania); MICINN (Spain); SNSF and SER (Switzerland); NASU (Ukraine); STFC (United Kingdom); DOE NP and NSF (USA). We acknowledge the computing resources that are provided by CERN, IN2P3 (France), KIT and DESY (Germany), INFN (Italy), SURF (Netherlands), PIC (Spain), GridPP (United Kingdom), CSCS (Switzerland), IFIN-HH (Romania), CBPF (Brazil), Polish WLCG (Poland) and NERSC (USA). We are indebted to the communities behind the multiple open-source software packages on which we depend. Individual groups or members have received support from ARC and ARDC (Australia); Minciencias (Colombia); AvH Foundation (Germany); EPLANET, Marie Skłodowska-Curie Actions and ERC (European Union); A\*MIDEX, ANR, IPhU and Labex P2IO, and Région Auvergne-Rhône-Alpes (France); Key Research Program of Frontier Sciences of CAS, CAS PIFI, CAS CCEPP, Fundamental Research Funds for the Central Universities, and Sci. & Tech. Program of Guangzhou (China); GVA, XuntaGal, GENCAT and Prog. Atracción Talento, CM (Spain); SRC (Sweden); the Leverhulme Trust, the Royal Society and UKRI (United Kingdom).

## References

- [1] E. Chapon *et al.*, *Prospects for quarkonium studies at the high-luminosity LHC*, Prog. Part. Nucl. Phys. **122** (2022) 103906, [arXiv:2012.14161](#).
- [2] C.-H. Chang, *Hadronic production of  $J/\psi$  associated with a gluon*, Nucl. Phys. **B172** (1980) 425.
- [3] E. L. Berger and D. L. Jones, *Inelastic photoproduction of  $J/\psi$  and  $\Upsilon$  by gluons*, Phys. Rev. **D23** (1981) 1521.
- [4] R. Baier and R. Ruckl, *Hadronic production of  $J/\psi$  and  $\Upsilon$ : transverse momentum distributions*, Phys. Lett. **B102** (1981) 364.
- [5] G. T. Bodwin, E. Braaten, and G. P. Lepage, *Rigorous QCD analysis of inclusive annihilation and production of heavy quarkonium*, Phys. Rev. **D51** (1995) 1125, Erratum *ibid.* **D55** (1997) 5853, [arXiv:hep-ph/9407339](#).
- [6] G. T. Bodwin, H. S. Chung, U.-R. Kim, and J. Lee, *Fragmentation contributions to  $J/\psi$  production at the Tevatron and the LHC*, Phys. Rev. Lett. **113** (2014) 022001, [arXiv:1403.3612](#).
- [7] E. Braaten, M. A. Doncheski, S. Fleming, and M. L. Mangano, *Fragmentation production of  $J/\psi$  and  $\psi'$  at the Tevatron*, Phys. Lett. **B333** (1994) 548, [arXiv:hep-ph/9405407](#).
- [8] P. L. Cho and A. K. Leibovich, *Color octet quarkonia production*, Phys. Rev. **D53** (1996) 150, [arXiv:hep-ph/9505329](#).
- [9] Y.-Q. Ma, K. Wang, and K.-T. Chao,  *$J/\psi(\psi')$  production at the Tevatron and LHC at  $\mathcal{O}(\alpha_s^4 v^4)$  in nonrelativistic QCD*, Phys. Rev. Lett. **106** (2011) 042002, [arXiv:1009.3655](#).
- [10] B. Gong, L.-P. Wan, J.-X. Wang, and H.-F. Zhang, *Polarization for prompt  $J/\psi$  and  $\psi(2S)$  production at the Tevatron and LHC*, Phys. Rev. Lett. **110** (2013) 042002, [arXiv:1205.6682](#).
- [11] M. Butenschoen and B. A. Kniehl, *Reconciling  $J/\psi$  production at HERA, RHIC, Tevatron, and LHC with NRQCD factorization at next-to-leading order*, Phys. Rev. Lett. **106** (2011) 022003, [arXiv:1009.5662](#).
- [12] H. S. Shao *et al.*, *Yields and polarizations of prompt  $J/\psi$  and  $\psi(2S)$  production in hadronic collisions*, JHEP **05** (2015) 103, [arXiv:1411.3300](#).
- [13] N. Brambilla *et al.*, *Heavy quarkonium: progress, puzzles, and opportunities*, Eur. Phys. J. **C71** (2011) 1534, [arXiv:1010.5827](#).
- [14] H. Han *et al.*,  *$\eta_c$  production at LHC and indications on the understanding of  $J/\psi$  production*, Phys. Rev. Lett. **114** (2015) 092005, [arXiv:1411.7350](#).
- [15] K.-T. Chao *et al.*,  *$J/\psi$  polarization at hadron colliders in nonrelativistic QCD*, Phys. Rev. Lett. **108** (2012) 242004, [arXiv:1201.2675](#).

- [16] H.-F. Zhang, Z. Sun, W.-L. Sang, and R. Li, *Impact of  $\eta_c$  hadroproduction data on charmonium production and polarization within NRQCD framework*, Phys. Rev. Lett. **114** (2015) 092006, [arXiv:1412.0508](#).
- [17] M. Butenschoen, Z.-G. He, and B. A. Kniehl,  *$\eta_c$  production at the LHC challenges nonrelativistic-QCD factorization*, Phys. Rev. Lett. **114** (2015) 092004, [arXiv:1411.5287](#).
- [18] E. Braaten, B. A. Kniehl, and J. Lee, *Polarization of prompt  $J/\psi$  at the Tevatron*, Phys. Rev. **D62** (2000) 094005, [arXiv:hep-ph/9911436](#).
- [19] LHCb collaboration, R. Aaij *et al.*, *Study of  $J/\psi$  production in jets*, Phys. Rev. Lett. **118** (2017) 192001, [arXiv:1701.05116](#).
- [20] H.-S. Shao and Y.-J. Zhang, *Complete study of hadroproduction of a  $\Upsilon$  meson associated with a prompt  $J/\psi$* , Phys. Rev. Lett. **117** (2016) 062001, [arXiv:1605.03061](#).
- [21] L.-P. Sun, H. Han, and K.-T. Chao, *Impact of  $J/\psi$  pair production at the LHC and predictions in nonrelativistic QCD*, Phys. Rev. **D94** (2016) 074033, [arXiv:1404.4042](#).
- [22] Y.-J. Li, G.-Z. Xu, K.-Y. Liu, and Y.-J. Zhang, *Relativistic correction to  $J/\psi$  and  $\Upsilon$  pair production*, JHEP **07** (2013) 051, [arXiv:1303.1383](#).
- [23] Z.-G. He, B. A. Kniehl, and X.-P. Wang, *Breakdown of nonrelativistic QCD factorization in processes involving two quarkonia and its cure*, Phys. Rev. Lett. **121** (2018) 172001, [arXiv:1809.07993](#).
- [24] G. Calucci and D. Treleani, *Minijets and the two-body parton correlation*, Phys. Rev. **D57** (1998) 503.
- [25] G. Calucci and D. Treleani, *Proton structure in transverse space and the effective cross section*, Phys. Rev. **D60** (1999) 054023.
- [26] A. Del Fabbro and D. Treleani, *Scale factor in double parton collisions and parton densities in transverse space*, Phys. Rev. **D63** (2001) 057901.
- [27] I. Belyaev and D. Savrina, *Study of double parton scattering processes with heavy quarks*, Adv. Ser. Direct. High Energy Phys. **29** (2018) 141, [arXiv:1711.10877](#).
- [28] J.-P. Lansberg and H.-S. Shao, *Associated production of a quarkonium and a  $Z$  boson at one loop in a quark-hadron-duality approach*, JHEP **10** (2016) 153, [arXiv:1608.03198](#).
- [29] J.-P. Lansberg, *New observables in inclusive production of quarkonia*, Phys. Rept. **889** (2020) 1, [arXiv:1903.09185](#).
- [30] J.-P. Lansberg and H.-S. Shao,  *$J/\psi$ -pair production at large momenta: indications for double parton scatterings and large  $\alpha_s^5$  contributions*, Phys. Lett. **B751** (2015) 479, [arXiv:1410.8822](#).
- [31] J.-P. Lansberg, H.-S. Shao, and N. Yamanaka, *Indication for double parton scatterings in  $W^+$  prompt  $J/\psi$  production at the LHC*, Phys. Lett. **B781** (2018) 485, [arXiv:1707.04350](#).

- [32] J.-P. Lansberg and H.-S. Shao, *Phenomenological analysis of associated production of  $Z^0 + b$  in the  $b \rightarrow J/\psi X$  decay channel at the LHC*, Nucl. Phys. **B916** (2017) 132, [arXiv:1611.09303](#).
- [33] D0 collaboration, V. M. Abazov *et al.*, *Observation and studies of double  $J/\psi$  production at the Tevatron*, Phys. Rev. **D90** (2014) 111101, [arXiv:1406.2380](#).
- [34] ATLAS collaboration, M. Aaboud *et al.*, *Measurement of the prompt  $J/\psi$  pair production cross-section in  $pp$  collisions at  $\sqrt{s} = 8$  TeV with the ATLAS detector*, Eur. Phys. J. **C77** (2017) 76, [arXiv:1612.02950](#).
- [35] ATLAS collaboration, G. Aad *et al.*, *Measurement of hard double-parton interactions in  $W(\rightarrow l\nu) + 2$  jet events at  $\sqrt{s}=7$  TeV with the ATLAS detector*, New J. Phys. **15** (2013) 033038, [arXiv:1301.6872](#).
- [36] CMS collaboration, S. Chatrchyan *et al.*, *Study of double parton scattering using  $W + 2$ -Jet events in proton-proton collisions at  $\sqrt{s} = 7$  TeV*, JHEP **03** (2014) 032, [arXiv:1312.5729](#).
- [37] LHCb collaboration, R. Aaij *et al.*, *Observation of double charm production involving open charm in  $pp$  collisions at  $\sqrt{s} = 7$  TeV*, JHEP **06** (2012) 141, Addendum *ibid.* **03** (2014) 108, [arXiv:1205.0975](#).
- [38] LHCb collaboration, R. Aaij *et al.*, *Production of associated  $\Upsilon$  and open charm hadrons in  $pp$  collisions at  $\sqrt{s} = 7$  and 8 TeV via double parton scattering*, JHEP **07** (2016) 052, [arXiv:1510.05949](#).
- [39] CDF collaboration, F. Abe *et al.*, *Study of four jet events and evidence for double parton interactions in  $p\bar{p}$  collisions at  $\sqrt{s} = 1.8$  TeV*, Phys. Rev. **D47** (1993) 4857.
- [40] CDF collaboration, F. Abe *et al.*, *Double parton scattering in  $p\bar{p}$  collisions at  $\sqrt{s} = 1.8$  TeV*, Phys. Rev. **D56** (1997) 3811.
- [41] D0 collaboration, V. M. Abazov *et al.*, *Double parton interactions in  $\gamma + 3$  jet events in  $p\bar{p}$  collisions at  $\sqrt{s}=1.96$  TeV*, Phys. Rev. **D81** (2010) 052012, [arXiv:0912.5104](#).
- [42] H.-S. Shao,  *$J/\psi$  meson production in association with an open charm hadron at the LHC: A reappraisal*, Phys. Rev. **D102** (2020) 034023, [arXiv:2005.12967](#).
- [43] NA3 collaboration, J. Badier *et al.*, *Evidence for  $\psi\psi$  production in  $\pi^-$  interactions at 150 and 280 GeV/c*, Phys. Lett. **B114** (1982) 457.
- [44] LHCb collaboration, R. Aaij *et al.*, *Observation of  $J/\psi$ -pair production in  $pp$  collisions at  $\sqrt{s} = 7$  TeV*, Phys. Lett. **B707** (2012) 52, [arXiv:1109.0963](#).
- [45] CMS collaboration, V. Khachatryan *et al.*, *Measurement of prompt  $J/\psi$  pair production in  $pp$  collisions at  $\sqrt{s} = 7$  TeV*, JHEP **09** (2014) 094, [arXiv:1406.0484](#).
- [46] LHCb collaboration, R. Aaij *et al.*, *Measurement of the  $J/\psi$  pair production cross-section in  $pp$  collisions at  $\sqrt{s} = 13$  TeV*, JHEP **06** (2017) 047, Erratum *ibid.* **10** (2017) 068, [arXiv:1612.07451](#).

- [47] LHCb collaboration, R. Aaij *et al.*, *Observation of structure in the  $J/\psi$ -pair mass spectrum*, Science Bulletin **65** (2020) 1983, [arXiv:2006.16957](#).
- [48] CMS collaboration, A. Hayrapetyan *et al.*, *Observation of new structures in the  $J/\psi J/\psi$  mass spectrum in pp collisions at  $\sqrt{s} = 13 \text{ TeV}$* , [arXiv:2306.07164](#).
- [49] ATLAS collaboration, G. Aad *et al.*, *Observation of an excess of di-charmonium events in the four-muon final state with the ATLAS detector*, [arXiv:2304.08962](#).
- [50] CMS collaboration, V. Khachatryan *et al.*, *Observation of  $\Upsilon(1S)$  pair production in proton-proton collisions at  $\sqrt{s} = 8 \text{ TeV}$* , JHEP **05** (2017) 013, [arXiv:1610.07095](#).
- [51] D0 collaboration, V. M. Abazov *et al.*, *Evidence for simultaneous production of  $J/\psi$  and  $\Upsilon$  mesons*, Phys. Rev. Lett. **116** (2016) 082002, [arXiv:1511.02428](#).
- [52] ALICE collaboration, B. Abelev *et al.*,  *$J/\psi$  polarization in pp collisions at  $\sqrt{s} = 7 \text{ TeV}$* , Phys. Rev. Lett. **108** (2012) 082001, [arXiv:1111.1630](#).
- [53] CMS collaboration, S. Chatrchyan *et al.*, *Measurement of the Prompt  $J/\psi$  and  $\psi(2S)$  Polarizations in pp Collisions at  $\sqrt{s} = 7 \text{ TeV}$* , Phys. Lett. B **727** (2013) 381, [arXiv:1307.6070](#).
- [54] CMS collaboration, S. Chatrchyan *et al.*, *Measurement of the  $\Upsilon(1S)$ ,  $\Upsilon(2S)$  and  $\Upsilon(3S)$  Polarizations in pp Collisions at  $\sqrt{s} = 7 \text{ TeV}$* , Phys. Rev. Lett. **110** (2013) 081802, [arXiv:1209.2922](#).
- [55] LHCb collaboration, R. Aaij *et al.*, *Measurement of  $J/\psi$  polarization in pp collisions at  $\sqrt{s} = 7 \text{ TeV}$* , Eur. Phys. J. **C73** (2013) 2631, [arXiv:1307.6379](#).
- [56] LHCb collaboration, R. Aaij *et al.*, *Measurement of  $\psi(2S)$  polarisation in pp collisions at  $\sqrt{s} = 7 \text{ TeV}$* , Eur. Phys. J. **C74** (2014) 2872, [arXiv:1403.1339](#).
- [57] LHCb collaboration, R. Aaij *et al.*, *Measurement of the  $\Upsilon(nS)$  polarizations in pp collisions at  $\sqrt{s} = 7$  and  $8 \text{ TeV}$* , JHEP **12** (2017) 110, [arXiv:1709.01301](#).
- [58] LHCb collaboration, A. A. Alves Jr. *et al.*, *The LHCb detector at the LHC*, JINST **3** (2008) S08005.
- [59] LHCb collaboration, R. Aaij *et al.*, *LHCb detector performance*, Int. J. Mod. Phys. **A30** (2015) 1530022, [arXiv:1412.6352](#).
- [60] R. Aaij *et al.*, *The LHCb trigger and its performance in 2011*, JINST **8** (2013) P04022, [arXiv:1211.3055](#).
- [61] T. Sjöstrand, S. Mrenna, and P. Skands, *A brief introduction to PYTHIA 8.1*, Comput. Phys. Commun. **178** (2008) 852, [arXiv:0710.3820](#).
- [62] I. Belyaev *et al.*, *Handling of the generation of primary events in Gauss, the LHCb simulation framework*, J. Phys. Conf. Ser. **331** (2011) 032047.
- [63] D. J. Lange, *The EvtGen particle decay simulation package*, Nucl. Instrum. Meth. **A462** (2001) 152.

- [64] P. Golonka and Z. Was, *PHOTOS Monte Carlo: A precision tool for QED corrections in  $Z$  and  $W$  decays*, Eur. Phys. J. **C45** (2006) 97, [arXiv:hep-ph/0506026](https://arxiv.org/abs/hep-ph/0506026).
- [65] Geant4 collaboration, J. Allison *et al.*, *Geant4 developments and applications*, IEEE Trans. Nucl. Sci. **53** (2006) 270; Geant4 collaboration, S. Agostinelli *et al.*, *Geant4: A simulation toolkit*, Nucl. Instrum. Meth. **A506** (2003) 250.
- [66] M. Clemencic *et al.*, *The LHCb simulation application, Gauss: Design, evolution and experience*, J. Phys. Conf. Ser. **331** (2011) 032023.
- [67] Particle Data Group, R. L. Workman *et al.*, *Review of particle physics*, Prog. Theor. Exp. Phys. **2022** (2022) 083C01.
- [68] S. van der Meer, *Calibration of the effective beam height in the ISR*, CERN-ISR-PO-68-31, 1968.
- [69] LHCb collaboration, R. Aaij *et al.*, *Precision luminosity measurements at LHCb*, JINST **9** (2014) P12005, [arXiv:1410.0149](https://arxiv.org/abs/1410.0149).
- [70] F. Archilli *et al.*, *Performance of the muon identification at LHCb*, JINST **8** (2013) P10020, [arXiv:1306.0249](https://arxiv.org/abs/1306.0249).
- [71] T. Skwarnicki, *A study of the radiative cascade transitions between the Upsilon-prime and Upsilon resonances*, PhD thesis, Institute of Nuclear Physics, Krakow, 1986, DESY-F31-86-02.
- [72] M. Pivk and F. R. Le Diberder, *sPlot: A statistical tool to unfold data distributions*, Nucl. Instrum. Meth. **A555** (2005) 356, [arXiv:physics/0402083](https://arxiv.org/abs/physics/0402083).
- [73] LHCb collaboration, R. Aaij *et al.*, *Measurement of forward  $J/\psi$  production cross-sections in  $pp$  collisions at  $\sqrt{s} = 13 \text{ TeV}$* , JHEP **10** (2015) 172, Erratum *ibid.* **05** (2017) 063, [arXiv:1509.00771](https://arxiv.org/abs/1509.00771).
- [74] LHCb collaboration, R. Aaij *et al.*, *Measurement of the track reconstruction efficiency at LHCb*, JINST **10** (2015) P02007, [arXiv:1408.1251](https://arxiv.org/abs/1408.1251).
- [75] S. Tolk, J. Albrecht, F. Dettori, and A. Pellegrino, *Data driven trigger efficiency determination at LHCb*, LHCb-PUB-2014-039, 2014.
- [76] LHCb collaboration, R. Aaij *et al.*, *Measurement of  $\Upsilon$  production cross-section in  $pp$  collisions at  $\sqrt{s} = 13 \text{ TeV}$* , JHEP **07** (2018) 134, [arXiv:1804.09214](https://arxiv.org/abs/1804.09214).



S. Didenko<sup>38</sup> ID, L. Dieste Maronas<sup>40</sup>, S. Ding<sup>62</sup> ID, V. Dobishuk<sup>46</sup> ID, A. Dolmatov<sup>38</sup>, C. Dong<sup>3</sup> ID, A.M. Donohoe<sup>18</sup> ID, F. Dordei<sup>27</sup> ID, A.C. dos Reis<sup>1</sup> ID, L. Douglas<sup>53</sup>, A.G. Downes<sup>8</sup> ID, P. Duda<sup>75</sup> ID, M.W. Dudek<sup>35</sup> ID, L. Dufour<sup>42</sup> ID, V. Duk<sup>72</sup> ID, P. Durante<sup>42</sup> ID, M. M. Duras<sup>75</sup> ID, J.M. Durham<sup>61</sup> ID, D. Dutta<sup>56</sup> ID, A. Dziurda<sup>35</sup> ID, A. Dzyuba<sup>38</sup> ID, S. Easo<sup>51</sup> ID, U. Egede<sup>63</sup> ID, V. Egorychev<sup>38</sup> ID, C. Eirea Orro<sup>40</sup>, S. Eisenhardt<sup>52</sup> ID, E. Ejopu<sup>56</sup> ID, S. Ek-In<sup>43</sup> ID, L. Eklund<sup>77</sup> ID, M.E Elashri<sup>59</sup> ID, J. Ellbracht<sup>15</sup> ID, S. Ely<sup>55</sup> ID, A. Ene<sup>37</sup> ID, E. Epple<sup>59</sup> ID, S. Escher<sup>14</sup> ID, J. Eschle<sup>44</sup> ID, S. Esen<sup>44</sup> ID, T. Evans<sup>56</sup> ID, F. Fabiano<sup>27,h</sup> ID, L.N. Falcao<sup>1</sup> ID, Y. Fan<sup>6</sup> ID, B. Fang<sup>11,68</sup> ID, L. Fantini<sup>72,p</sup> ID, M. Faria<sup>43</sup> ID, S. Farry<sup>54</sup> ID, D. Fazzini<sup>26,m</sup> ID, L.F Felkowski<sup>75</sup> ID, M. Feo<sup>42</sup> ID, M. Fernandez Gomez<sup>40</sup> ID, A.D. Fernez<sup>60</sup> ID, F. Ferrari<sup>20</sup> ID, L. Ferreira Lopes<sup>43</sup> ID, F. Ferreira Rodrigues<sup>2</sup> ID, S. Ferreres Sole<sup>32</sup> ID, M. Ferrillo<sup>44</sup> ID, M. Ferro-Luzzi<sup>42</sup> ID, S. Filippov<sup>38</sup> ID, R.A. Fini<sup>19</sup> ID, M. Fiorini<sup>21,i</sup> ID, M. Firlej<sup>34</sup> ID, K.M. Fischer<sup>57</sup> ID, D.S. Fitzgerald<sup>78</sup> ID, C. Fitzpatrick<sup>56</sup> ID, T. Fiutowski<sup>34</sup> ID, F. Fleuret<sup>12</sup> ID, M. Fontana<sup>13</sup> ID, F. Fontanelli<sup>24,k</sup> ID, R. Forty<sup>42</sup> ID, D. Foulds-Holt<sup>49</sup> ID, V. Franco Lima<sup>54</sup> ID, M. Franco Sevilla<sup>60</sup> ID, M. Frank<sup>42</sup> ID, E. Franzoso<sup>21,i</sup> ID, G. Frau<sup>17</sup> ID, C. Frei<sup>42</sup> ID, D.A. Friday<sup>56</sup> ID, L.F Frontini<sup>25,l</sup> ID, J. Fu<sup>6</sup> ID, Q. Fuehring<sup>15</sup> ID, T. Fulghesu<sup>13</sup> ID, E. Gabriel<sup>32</sup> ID, G. Galati<sup>19,f</sup> ID, M.D. Galati<sup>32</sup> ID, A. Gallas Torreira<sup>40</sup> ID, D. Galli<sup>20,g</sup> ID, S. Gambetta<sup>52,42</sup> ID, M. Gandelman<sup>2</sup> ID, P. Gandini<sup>25</sup> ID, H.G Gao<sup>6</sup> ID, Y. Gao<sup>7</sup> ID, Y. Gao<sup>5</sup> ID, M. Garau<sup>27,h</sup> ID, L.M. Garcia Martin<sup>50</sup> ID, P. Garcia Moreno<sup>39</sup> ID, J. García Pardiñas<sup>42</sup> ID, B. Garcia Plana<sup>40</sup>, F.A. Garcia Rosales<sup>12</sup> ID, L. Garrido<sup>39</sup> ID, C. Gaspar<sup>42</sup> ID, R.E. Geertsema<sup>32</sup> ID, D. Gerick<sup>17</sup>, L.L. Gerken<sup>15</sup> ID, E. Gersabeck<sup>56</sup> ID, M. Gersabeck<sup>56</sup> ID, T. Gershon<sup>50</sup> ID, L. Giambastiani<sup>28</sup> ID, V. Gibson<sup>49</sup> ID, H.K. Giemza<sup>36</sup> ID, A.L. Gilman<sup>57</sup> ID, M. Giovannetti<sup>23</sup> ID, A. Gioventù<sup>40</sup> ID, P. Gironella Gironell<sup>39</sup> ID, C. Giugliano<sup>21,i</sup> ID, M.A. Giza<sup>35</sup> ID, K. Gizzdov<sup>52</sup> ID, E.L. Gkougkousis<sup>42</sup> ID, V.V. Gligorov<sup>13,42</sup> ID, C. Göbel<sup>64</sup> ID, E. Golobardes<sup>76</sup> ID, D. Golubkov<sup>38</sup> ID, A. Golutvin<sup>55,38</sup> ID, A. Gomes<sup>1,a</sup> ID, S. Gomez Fernandez<sup>39</sup> ID, F. Goncalves Abrantes<sup>57</sup> ID, M. Goncerz<sup>35</sup> ID, G. Gong<sup>3</sup> ID, I.V. Gorelov<sup>38</sup> ID, C. Gotti<sup>26</sup> ID, J.P. Grabowski<sup>70</sup> ID, T. Grammatico<sup>13</sup> ID, L.A. Granado Cardoso<sup>42</sup> ID, E. Graugés<sup>39</sup> ID, E. Graverini<sup>43</sup> ID, G. Graziani ID, A. T. Grecu<sup>37</sup> ID, L.M. Greeven<sup>32</sup> ID, N.A. Grieser<sup>59</sup> ID, L. Grillo<sup>53</sup> ID, S. Gromov<sup>38</sup> ID, B.R. Gruberg Cazon<sup>57</sup> ID, C. Gu<sup>3</sup> ID, M. Guarise<sup>21,i</sup> ID, M. Guittiere<sup>11</sup> ID, P. A. Günther<sup>17</sup> ID, E. Gushchin<sup>38</sup> ID, A. Guth<sup>14</sup>, Y. Guz<sup>5,38,42</sup> ID, T. Gys<sup>42</sup> ID, T. Hadavizadeh<sup>63</sup> ID, C. Hadjivasilou<sup>60</sup> ID, G. Haefeli<sup>43</sup> ID, C. Haen<sup>42</sup> ID, J. Haimberger<sup>42</sup> ID, S.C. Haines<sup>49</sup> ID, T. Halewood-leagas<sup>54</sup> ID, M.M. Halvorsen<sup>42</sup> ID, P.M. Hamilton<sup>60</sup> ID, J. Hammerich<sup>54</sup> ID, Q. Han<sup>7</sup> ID, X. Han<sup>17</sup> ID, S. Hansmann-Menzemer<sup>17</sup> ID, L. Hao<sup>6</sup> ID, N. Harnew<sup>57</sup> ID, T. Harrison<sup>54</sup> ID, C. Hasse<sup>42</sup> ID, M. Hatch<sup>42</sup> ID, J. He<sup>6,c</sup> ID, K. Heijhoff<sup>32</sup> ID, F.H Hemmer<sup>42</sup> ID, C. Henderson<sup>59</sup> ID, R.D.L. Henderson<sup>63,50</sup> ID, A.M. Hennequin<sup>58</sup> ID, K. Hennessy<sup>54</sup> ID, L. Henry<sup>42</sup> ID, J.H Herd<sup>55</sup> ID, J. Heuel<sup>14</sup> ID, A. Hicheur<sup>2</sup> ID, D. Hill<sup>43</sup> ID, M. Hilton<sup>56</sup> ID, S.E. Hollitt<sup>15</sup> ID, J. Horswill<sup>56</sup> ID, R. Hou<sup>7</sup> ID, Y. Hou<sup>8</sup> ID, J. Hu<sup>17</sup>, J. Hu<sup>66</sup> ID, W. Hu<sup>5</sup> ID, X. Hu<sup>3</sup> ID, W. Huang<sup>6</sup> ID, X. Huang<sup>68</sup>, W. Hulsbergen<sup>32</sup> ID, R.J. Hunter<sup>50</sup> ID, M. Hushchyn<sup>38</sup> ID, D. Hutchcroft<sup>54</sup> ID, P. Ibis<sup>15</sup> ID, M. Idzik<sup>34</sup> ID, D. Ilin<sup>38</sup> ID, P. Ilten<sup>59</sup> ID, A. Inglessi<sup>38</sup> ID, A. Iniuikhin<sup>38</sup> ID, A. Ishteev<sup>38</sup> ID, K. Ivshin<sup>38</sup> ID, R. Jacobsson<sup>42</sup> ID, H. Jage<sup>14</sup> ID, S.J. Jaimes Elles<sup>41</sup> ID, S. Jakobsen<sup>42</sup> ID, E. Jans<sup>32</sup> ID, B.K. Jashal<sup>41</sup> ID, A. Jawahery<sup>60</sup> ID, V. Jevtic<sup>15</sup> ID, E. Jiang<sup>60</sup> ID, X. Jiang<sup>4,6</sup> ID, Y. Jiang<sup>6</sup> ID, M. John<sup>57</sup> ID, D. Johnson<sup>58</sup> ID, C.R. Jones<sup>49</sup> ID, T.P. Jones<sup>50</sup> ID, S.J Joshi<sup>36</sup> ID, B. Jost<sup>42</sup> ID, N. Jurik<sup>42</sup> ID, I. Juszczak<sup>35</sup> ID, S. Kandybei<sup>45</sup> ID, Y. Kang<sup>3</sup> ID, M. Karacson<sup>42</sup> ID, D. Karpenkov<sup>38</sup> ID, M. Karpov<sup>38</sup> ID, J.W. Kautz<sup>59</sup> ID, F. Keizer<sup>42</sup> ID, D.M. Keller<sup>62</sup> ID, M. Kenzie<sup>50</sup> ID, T. Ketel<sup>32</sup> ID, B. Khanji<sup>15</sup> ID, A. Kharisova<sup>38</sup> ID, S. Kholodenko<sup>38</sup> ID, G. Khreich<sup>11</sup> ID, T. Kirn<sup>14</sup> ID, V.S. Kirsebom<sup>43</sup> ID, O. Kitouni<sup>58</sup> ID, S. Klaver<sup>33</sup> ID, N. Kleijne<sup>29,q</sup> ID, K. Klimaszewski<sup>36</sup> ID, M.R. Kmiec<sup>36</sup> ID, S. Koliiev<sup>46</sup> ID, L. Kolk<sup>15</sup> ID, A. Kondybayeva<sup>38</sup> ID, A. Konoplyannikov<sup>38</sup> ID, P. Kopciewicz<sup>34</sup> ID, R. Kopecna<sup>17</sup>, P. Koppenburg<sup>32</sup> ID, M. Korolev<sup>38</sup> ID, I. Kostiuk<sup>32</sup> ID, O. Kot<sup>46</sup>, S. Kotriakhova ID, A. Kozachuk<sup>38</sup> ID, P. Kravchenko<sup>38</sup> ID, L. Kravchuk<sup>38</sup> ID, R.D. Krawczyk<sup>42</sup> ID,





F.F. Wilson<sup>51</sup> , W. Wislicki<sup>36</sup> , M. Witek<sup>35</sup> , L. Witola<sup>17</sup> , C.P. Wong<sup>61</sup> ,  
G. Wormser<sup>11</sup> , S.A. Wotton<sup>49</sup> , H. Wu<sup>62</sup> , J. Wu<sup>7</sup> , K. Wyllie<sup>42</sup> , Z. Xiang<sup>6</sup> ,  
Y. Xie<sup>7</sup> , A. Xu<sup>5</sup> , J. Xu<sup>6</sup> , L. Xu<sup>3</sup> , L. Xu<sup>3</sup> , M. Xu<sup>50</sup> , Q. Xu<sup>6</sup>, Z. Xu<sup>9</sup> , Z. Xu<sup>6</sup> ,  
D. Yang<sup>3</sup> , S. Yang<sup>6</sup> , X. Yang<sup>5</sup> , Y. Yang<sup>6</sup> , Z. Yang<sup>5</sup> , Z. Yang<sup>60</sup> ,  
L.E. Yeomans<sup>54</sup> , V. Yeroshenko<sup>11</sup> , H. Yeung<sup>56</sup> , H. Yin<sup>7</sup> , J. Yu<sup>65</sup> , X. Yuan<sup>62</sup> ,  
E. Zaffaroni<sup>43</sup> , M. Zavertyaev<sup>16</sup> , M. Zdybal<sup>35</sup> , M. Zeng<sup>3</sup> , C. Zhang<sup>5</sup> , D. Zhang<sup>7</sup> ,  
L. Zhang<sup>3</sup> , S. Zhang<sup>65</sup> , S. Zhang<sup>5</sup> , Y. Zhang<sup>5</sup> , Y. Zhang<sup>57</sup> , Y. Zhao<sup>17</sup> ,  
A. Zharkova<sup>38</sup> , A. Zhelezov<sup>17</sup> , Y. Zheng<sup>6</sup> , T. Zhou<sup>5</sup> , X. Zhou<sup>7</sup> , Y. Zhou<sup>6</sup> ,  
V. Zhovkovska<sup>11</sup> , X. Zhu<sup>3</sup> , X. Zhu<sup>7</sup> , Z. Zhu<sup>6</sup> , V. Zhukov<sup>14,38</sup> , Q. Zou<sup>4,6</sup> ,  
S. Zucchelli<sup>20,g</sup> , D. Zuliani<sup>28</sup> , G. Zunică<sup>56</sup> .

<sup>1</sup>*Centro Brasileiro de Pesquisas Físicas (CBPF), Rio de Janeiro, Brazil*

<sup>2</sup>*Universidade Federal do Rio de Janeiro (UFRJ), Rio de Janeiro, Brazil*

<sup>3</sup>*Center for High Energy Physics, Tsinghua University, Beijing, China*

<sup>4</sup>*Institute Of High Energy Physics (IHEP), Beijing, China*

<sup>5</sup>*School of Physics State Key Laboratory of Nuclear Physics and Technology, Peking University, Beijing, China*

<sup>6</sup>*University of Chinese Academy of Sciences, Beijing, China*

<sup>7</sup>*Institute of Particle Physics, Central China Normal University, Wuhan, Hubei, China*

<sup>8</sup>*Université Savoie Mont Blanc, CNRS, IN2P3-LAPP, Annecy, France*

<sup>9</sup>*Université Clermont Auvergne, CNRS/IN2P3, LPC, Clermont-Ferrand, France*

<sup>10</sup>*Aix Marseille Univ, CNRS/IN2P3, CPPM, Marseille, France*

<sup>11</sup>*Université Paris-Saclay, CNRS/IN2P3, IJCLab, Orsay, France*

<sup>12</sup>*Laboratoire Leprince-Ringuet, CNRS/IN2P3, Ecole Polytechnique, Institut Polytechnique de Paris, Palaiseau, France*

<sup>13</sup>*LPNHE, Sorbonne Université, Paris Diderot Sorbonne Paris Cité, CNRS/IN2P3, Paris, France*

<sup>14</sup>*I. Physikalisches Institut, RWTH Aachen University, Aachen, Germany*

<sup>15</sup>*Fakultät Physik, Technische Universität Dortmund, Dortmund, Germany*

<sup>16</sup>*Max-Planck-Institut für Kernphysik (MPIK), Heidelberg, Germany*

<sup>17</sup>*Physikalisch Institut, Ruprecht-Karls-Universität Heidelberg, Heidelberg, Germany*

<sup>18</sup>*School of Physics, University College Dublin, Dublin, Ireland*

<sup>19</sup>*INFN Sezione di Bari, Bari, Italy*

<sup>20</sup>*INFN Sezione di Bologna, Bologna, Italy*

<sup>21</sup>*INFN Sezione di Ferrara, Ferrara, Italy*

<sup>22</sup>*INFN Sezione di Firenze, Firenze, Italy*

<sup>23</sup>*INFN Laboratori Nazionali di Frascati, Frascati, Italy*

<sup>24</sup>*INFN Sezione di Genova, Genova, Italy*

<sup>25</sup>*INFN Sezione di Milano, Milano, Italy*

<sup>26</sup>*INFN Sezione di Milano-Bicocca, Milano, Italy*

<sup>27</sup>*INFN Sezione di Cagliari, Monserrato, Italy*

<sup>28</sup>*Università degli Studi di Padova, Università e INFN, Padova, Padova, Italy*

<sup>29</sup>*INFN Sezione di Pisa, Pisa, Italy*

<sup>30</sup>*INFN Sezione di Roma La Sapienza, Roma, Italy*

<sup>31</sup>*INFN Sezione di Roma Tor Vergata, Roma, Italy*

<sup>32</sup>*Nikhef National Institute for Subatomic Physics, Amsterdam, Netherlands*

<sup>33</sup>*Nikhef National Institute for Subatomic Physics and VU University Amsterdam, Amsterdam, Netherlands*

<sup>34</sup>*AGH - University of Science and Technology, Faculty of Physics and Applied Computer Science, Kraków, Poland*

<sup>35</sup>*Henryk Niewodniczanski Institute of Nuclear Physics Polish Academy of Sciences, Kraków, Poland*

<sup>36</sup>*National Center for Nuclear Research (NCBJ), Warsaw, Poland*

<sup>37</sup>*Horia Hulubei National Institute of Physics and Nuclear Engineering, Bucharest-Magurele, Romania*

<sup>38</sup>*Affiliated with an institute covered by a cooperation agreement with CERN*

<sup>39</sup>*ICCUB, Universitat de Barcelona, Barcelona, Spain*

<sup>40</sup>*Instituto Galego de Física de Altas Enerxías (IGFAE), Universidade de Santiago de Compostela, Santiago de Compostela, Spain*

- <sup>41</sup>*Instituto de Fisica Corpuscular, Centro Mixto Universidad de Valencia - CSIC, Valencia, Spain*
- <sup>42</sup>*European Organization for Nuclear Research (CERN), Geneva, Switzerland*
- <sup>43</sup>*Institute of Physics, Ecole Polytechnique Fédérale de Lausanne (EPFL), Lausanne, Switzerland*
- <sup>44</sup>*Physik-Institut, Universität Zürich, Zürich, Switzerland*
- <sup>45</sup>*NSC Kharkiv Institute of Physics and Technology (NSC KIPT), Kharkiv, Ukraine*
- <sup>46</sup>*Institute for Nuclear Research of the National Academy of Sciences (KINR), Kyiv, Ukraine*
- <sup>47</sup>*University of Birmingham, Birmingham, United Kingdom*
- <sup>48</sup>*H.H. Wills Physics Laboratory, University of Bristol, Bristol, United Kingdom*
- <sup>49</sup>*Cavendish Laboratory, University of Cambridge, Cambridge, United Kingdom*
- <sup>50</sup>*Department of Physics, University of Warwick, Coventry, United Kingdom*
- <sup>51</sup>*STFC Rutherford Appleton Laboratory, Didcot, United Kingdom*
- <sup>52</sup>*School of Physics and Astronomy, University of Edinburgh, Edinburgh, United Kingdom*
- <sup>53</sup>*School of Physics and Astronomy, University of Glasgow, Glasgow, United Kingdom*
- <sup>54</sup>*Oliver Lodge Laboratory, University of Liverpool, Liverpool, United Kingdom*
- <sup>55</sup>*Imperial College London, London, United Kingdom*
- <sup>56</sup>*Department of Physics and Astronomy, University of Manchester, Manchester, United Kingdom*
- <sup>57</sup>*Department of Physics, University of Oxford, Oxford, United Kingdom*
- <sup>58</sup>*Massachusetts Institute of Technology, Cambridge, MA, United States*
- <sup>59</sup>*University of Cincinnati, Cincinnati, OH, United States*
- <sup>60</sup>*University of Maryland, College Park, MD, United States*
- <sup>61</sup>*Los Alamos National Laboratory (LANL), Los Alamos, NM, United States*
- <sup>62</sup>*Syracuse University, Syracuse, NY, United States*
- <sup>63</sup>*School of Physics and Astronomy, Monash University, Melbourne, Australia, associated to <sup>50</sup>*
- <sup>64</sup>*Pontifícia Universidade Católica do Rio de Janeiro (PUC-Rio), Rio de Janeiro, Brazil, associated to <sup>2</sup>*
- <sup>65</sup>*Physics and Micro Electronic College, Hunan University, Changsha City, China, associated to <sup>7</sup>*
- <sup>66</sup>*Guangdong Provincial Key Laboratory of Nuclear Science, Guangdong-Hong Kong Joint Laboratory of Quantum Matter, Institute of Quantum Matter, South China Normal University, Guangzhou, China, associated to <sup>3</sup>*
- <sup>67</sup>*Lanzhou University, Lanzhou, China, associated to <sup>4</sup>*
- <sup>68</sup>*School of Physics and Technology, Wuhan University, Wuhan, China, associated to <sup>3</sup>*
- <sup>69</sup>*Departamento de Física, Universidad Nacional de Colombia, Bogota, Colombia, associated to <sup>13</sup>*
- <sup>70</sup>*Universität Bonn - Helmholtz-Institut für Strahlen und Kernphysik, Bonn, Germany, associated to <sup>17</sup>*
- <sup>71</sup>*Eotvos Lorand University, Budapest, Hungary, associated to <sup>42</sup>*
- <sup>72</sup>*INFN Sezione di Perugia, Perugia, Italy, associated to <sup>21</sup>*
- <sup>73</sup>*Van Swinderen Institute, University of Groningen, Groningen, Netherlands, associated to <sup>32</sup>*
- <sup>74</sup>*Universiteit Maastricht, Maastricht, Netherlands, associated to <sup>32</sup>*
- <sup>75</sup>*Faculty of Material Engineering and Physics, Cracow, Poland, associated to <sup>35</sup>*
- <sup>76</sup>*DS4DS, La Salle, Universitat Ramon Llull, Barcelona, Spain, associated to <sup>39</sup>*
- <sup>77</sup>*Department of Physics and Astronomy, Uppsala University, Uppsala, Sweden, associated to <sup>53</sup>*
- <sup>78</sup>*University of Michigan, Ann Arbor, MI, United States, associated to <sup>62</sup>*

<sup>a</sup>*Universidade de Brasília, Brasília, Brazil*

<sup>b</sup>*Central South U., Changsha, China*

<sup>c</sup>*Hangzhou Institute for Advanced Study, UCAS, Hangzhou, China*

<sup>d</sup>*Excellence Cluster ORIGINS, Munich, Germany*

<sup>e</sup>*Universidad Nacional Autónoma de Honduras, Tegucigalpa, Honduras*

<sup>f</sup>*Università di Bari, Bari, Italy*

<sup>g</sup>*Università di Bologna, Bologna, Italy*

<sup>h</sup>*Università di Cagliari, Cagliari, Italy*

<sup>i</sup>*Università di Ferrara, Ferrara, Italy*

<sup>j</sup>*Università di Firenze, Firenze, Italy*

<sup>k</sup>*Università di Genova, Genova, Italy*

<sup>l</sup>*Università degli Studi di Milano, Milano, Italy*

<sup>m</sup>*Università di Milano Bicocca, Milano, Italy*

<sup>n</sup>*Università di Modena e Reggio Emilia, Modena, Italy*

<sup>o</sup>*Università di Padova, Padova, Italy*

<sup>p</sup>*Università di Perugia, Perugia, Italy*

<sup>q</sup>*Scuola Normale Superiore, Pisa, Italy*

<sup>r</sup>*Università di Pisa, Pisa, Italy*

<sup>s</sup>*Università della Basilicata, Potenza, Italy*

<sup>t</sup>*Università di Roma Tor Vergata, Roma, Italy*

<sup>u</sup>*Università di Urbino, Urbino, Italy*

<sup>v</sup>*MSU - Iligan Institute of Technology (MSU-IIT), Iligan, Philippines*

<sup>w</sup>*Universidad de Alcalá, Alcalá de Henares , Spain*

<sup>†</sup>*Deceased*